Soret and Dufour Effects on Unsteady MHD Heat and Mass Transfer from a Permeable Stretching Sheet with Thermophoresis and Non-Uniform Heat Generation/Absorption

P. S. Reddy[1†] and A. J. Chamkha[1]

[1]Department of Mathematics, RGM College of Engg. and *Tech, Nandyal-518501, AP, India,*
[2]Mechanical Engineering Department, Prince Mohammad Bin Fahd University, Al-Khobar31952, Kingdom of Saudi Arabia.

†*Corresponding Author Email: suda1983@gmail.com*

ABSTRACT

This paper is focused on the study of heat and mass transfer characteristics of an unsteady MHD boundary layer flow through porous medium over a stretching sheet in the presence of thermo-diffusion and diffusion-thermo effects with thermophoresis, thermal radiation and non-uniform heat source/sink. The transformed conservation equations are solved numerically subject to the boundary conditions using an optimized, extensively validated, variational finite element analysis. The numerical code is validated with previous studies on special cases of the problem. The influence of important non-dimensional parameters, namely suction parameter (f_w), magnetic parameter (M), unsteadiness parameter (α), Soret parameter (Sr), Dufour parameter (Du) thermophoretic parameter (τ), space dependent (A1) and temperature dependent parameters (B1) and radiation parameter(An) on the velocity, temperature and concentration fields as well as the skin-friction coefficient, Nusselt number and Sherwood number are examined in detail and the results are shown graphically and in tabular form to know the physical importance of the problem. It is found that the imposition of wall fluid suction (f_w>0) in the flow problem has the effect of depreciating the velocity, temperature and concentration boundary layer thicknesses at every finite value of η. This deceleration in momentum, thermal and concentration profiles is because of the fact that suction is taken away the warm fluid from the surface of the stretching sheet.

Keywords: Stretching sheet; Soret and dufour effects; Thermophoresis; MHD; Heat source/sink; Finite element method.

NOMENCLATURE

A1	coefficient of space-dependent heat source/sink	q_r	radiative heat flux
		q'''	non-uniform heat source/sink
a, c	empirical constant	Re_x	local Reynolds number
B1	coefficient of temperature-dependent heat source/sink	Sc	Schmidt number
		Sh_x	Sherwood number
C	concentration of the species	Sr	Soret number
c_p	specific heat at constant pressure	t	time
c_s	concentration susceptibility	T	temperature of the fluid
C_w	uniform constant concentration	T_m	mean fluid temperature
C_∞	free stream concentration	T_w	uniform constant temperature
C_f	skin-friction coefficient	T_∞	free stream temperature
D_m	mass diffusion coefficient	U_w	stretching surface velocity
Du	Dufour number	u	velocity in the x-direction
f_w	dimensionless suction velocity	V_t	thermophoretic velocity
K1	permeability parameter	v	velocity in the y-direction
k_t	thermal diffusion ratio		
M	magnetic parameter	μ	dynamic viscosity
Nu_x	Nusselt number	θ	non-dimensional temperature
Pr	Prandtl number	σ^*	Stephan-Boltzman constant

σ	electrical conductivity	κ	thermal conductivity
α	unsteadiness parameter	η	similarity variable
τ	thermophoretic parameter	φ	non-dimensional concentration
ν	kinematic viscosity		
ρ	density of the fluid		

1. INTRODUCTION

The problem of two dimensional boundary layer flow, heat and mass transfer over a continuous stretching heated surface through porous medium finds numerous and wide range of applications in many engineering and manufacturing disciplines. For example, in a melt spinning process, the extrudate from the die is generally drawn and simultaneously stretched into a sheet or filament, which is thereafter solidified through rapid quenching or gradual cooling by direct contact with water or chilled metal rolls. In fact, stretching will bring in a unidirectional orientation to the extrudate, thereby improving the quality of the final product considerably which greatly depends on the flow, heat and mass transfer mechanism. Glass blowing, extrusion process, melt-spinning, food-stuff processing, design of heat exchangers, wire and fiber coating, glass-fiber production, manufacture of plastic and rubber sheets, cooling of a large metallic plate in a bath and continuous casting are the other areas where this kind of problems has applications.

In industry, polymer sheets and filaments are manufactured by continuous extrusion of the polymer from a die. The thin polymer sheet constitutes a continuously moving surface with a non-uniform velocity through an ambient fluid. The problem of heat and mass transfer flow due to stretching sheet has been implemented on many flow situations. The problem of steady two-dimensional viscous incompressible fluid caused by a stretching sheet was first examined by Sikiadis (1961). The thermal behavior of the problem was experimentally verified by Tsou *et al.* (1967). Later, Crane (1970) has expended the problem of Sikiadis (1961) in which he studied the flow past a stretching plate by taking linearly varying velocity with a distance from a fixed point. Gupta *et al.* (1977) have studied the heat and mass transfer characteristics of a fluid over a stretching sheet with suction or blowing. Grubka and Bobba (1985) studied the heat transfer characteristics over a continuous stretching surface with variable temperature. Ali (1994) has investigated flow and heat transfer characteristics on a continuous stretching surface using power-law velocity and temperature distributions. Vajravelu (1994) has analyzed the study of flow and heat transfer in a saturated porous medium over an impermeable stretching sheet. Two cases have been discussed in this problem, (i) the sheet with prescribed sheet temperature (PST-case) and (ii) the sheet with prescribed wall heat flux (PHF-case).

In all the previous investigations, the effects thermal radiation and magnetic field on the flow and heat transfer have not been studied. It is well known fact that radiative heat transfer flow is very important in manufacturing industries for the design of reliable equipment's, nuclear plants, gas turbines and various propulsion devices for aircraft, missiles, satellites and space vehicles. Also, the effects of thermal radiation on forced and free convection flow are important in the content of space technology and process involving high temperature. It is known fact that, the transverse magnetic field has specific industrial applications in polymer processing technology. Plumb *et al.* (1981) was the first to examine the effect of horizontal cross-flow and radiation on natural convection from vertical heated surface in a saturated porous media. Recently, Pal D *et al.* (2010) has discussed radiation effect on hydro magnetic Darcy-Forchheimer mixed convention flow over stretching sheet. Mansour and El-Shaer (2001) analyzed the effects of thermal radiation on magneto hydrodynamic natural convection flows in a fluid-saturated porous media. Pal (2005) studied heat and mass transfer in stagnation-point flow toward a stretching sheet in the presence of buoyancy force and thermal radiation. Vajravelu and Rollins (1992) studied heat transfer in electrically conducting fluid over a stretching sheet by taking into account of magnetic field only. Molla *et al.* (2011) studied the effect of thermal radiation on a steady two-dimensional natural convection laminar flow of viscous incompressible optically thick fluid along a vertical flat plate with streamwise sinusoidal surface temperature. Abo-Eldahab and El-Gendy (2004) investigated the problem of free convection heat transfer characteristics in an electrically conducting fluid near an isothermal sheet to study the combined effect of buoyancy and radiation in the presence of uniform transverse magnetic field.

In recent years, it is found that thermophoresis is a phenomenon and has many practical applications in removing small particles from gas streams, in determining exhaust gas particle trajectories from combustion devices, and in studying the particulate material deposition on turbine blades. It has been found that thermophoresis is the dominant mass transfer mechanism in the modified chemical vapor deposition (MCVD) process as currently used in the fabrication of optical fiber performs. Thermophoretic deposition of radioactive particles is considered to be one of the important factors causing accidents in nuclear reactors. A number of analytical and experimental papers in thermophoretic heat and mass transfer have been communicated. Talbot *et al.* (1980) presented a seminal study, considering boundary layer flow with thermophoretic effects, which has become a benchmark for subsequent studies. Several authors, Duwairi and Damseh 2008), Damseh *et al.* (2009), Mahdy and Hady (2009), Liu *et al.* (2009), Postelnicu (2007), Dinesh and Jayaraj (2009), Grosan *et al.* (2009),Tsai and Huang (2010) have investigated the influence of thermophoresis over a vertical plate, micro-channel, horizontal plate

and parallel plate, etc.

Soret and Dufour effects are very significant in both Newtonian and non-Newtonian fluids when density differences exist in flow regime. The thermo-diffusion (Soret) effect is corresponds to species differentiation developing in an initial homogeneous mixture submitted to a thermal gradient and the diffusion-thermo (Dufour) effect corresponds to the heat flux produced by a concentration gradient. Usually, in heat and mass transfer problems the variation of density with temperature and concentration give rise to a combined buoyancy force under natural convection and hence the temperature and concentration will influence the diffusion and energy of the species. Many papers are found in literature on Soret and Dufour effects on different geometries. Dulal Pal *et al.*(2014) has studied non-Darcian mixed convection heat and mass transfer flow over a stretching sheet with Soret - Dufour effect sohmic heating and viscous dissipation. MHD mixed convection flow with Soret and Dufour effects past a vertical plate embedded in porous medium was studied by Makinde (2011). Reddy *et al.* (2012) has presented finite element solution to the heat and mass transfer flow past a cylindrical annulus with Soret and Dufour effects. Recently, Chamkha *et al.* (2014) has studied the influence of Soret and Dufour effects on unsteady heat and mass transfer flow over a rotating vertical cone and they suggested that temperature and concentration fields are more influenced with the values of Soret and Dufour parameter.

In all the above studies, the physical situation is related to the process of uniform stretching sheet. For the development of more physically realistic characterization of the flow configuration it is very useful to introduce unsteadiness into the flow, heat and mass transfer problems. Very few studies have been found in literature on unsteady boundary flows over a stretching sheet. Wang (1990) was first studied the unsteady boundary layer flow of a liquid film over a stretching sheet. Later, Elbashbeshy and Bazid (2004) have presented the heat transfer over an unsteady stretching surface. Tsai *et al.* (2008) has discussed flow and heat transfer characteristics over an unsteady stretching surface by taking heat source into the account. Ishak *et al.* (2009) analyzed the effect of prescribed wall temperature on heat transfer flow over an unsteady stretching permeable surface. Ishak (2010) has presented unsteady MHD flow and heat transfer behavior over a stretching plate. Recently, Dulalpal (2011) has described the analysis of flow and heat transfer over an unsteady stretching surface with non-uniform heat source/sink and thermal radiation. Chamkha *et al.* (2001, 2010, 2011a, 2011b) have discussed unsteady three-dimensional heat and mass transfer flow with heat generation/absorption.

To the best of the authors' knowledge, no studies have been made to analyze the combined influence of Soret and Dufour effects on unsteady heat and mass transfer flow of a viscous incompressible electrically conducting fluid over a stretching sheet with thermal radiation, non-uniform heat source/sink and thermophoresis particle deposition. Hence, this problem is addressed in this paper. The conservation of mass, momentum, energy and diffusion equations

were transformed into a two-point boundary value problem. In this article, we employ an extensively validated, highly efficient, variational finite-element method to study the effect of unsteadiness on heat and mass transfer flow in a porous medium past a semi-infinite stretching sheet. The problem presented here has many practical applications, such as, technological, manufacturing industries, MHD generators, plasma studies, nuclear reactors, geothermal energy extractions and polymer extrusion.

2. FORMULATION OF THE PROBLEM

Consider a two-dimensional unsteady laminar boundary layer flow of viscous incompressible fluid over a continuous moving stretching sheet which issue from a thin slot. The coordinate system is such that x-axis is taken along the stretching surface in the direction of the motion with the slot at origin, and the y-axis is perpendicular to the surface of the sheet as shown schematically in Fig.1. A uniform transverse magnetic field $B(x)$ is applied along the y-axis. The surface of the sheet is maintained at uniform temperature and concentration, T_w and C_w, respectively, and these values are assumed to be greater than the ambient temperature and concentration, T_∞ and C_∞, respectively. The flow is assumed to be confined in a region $y > 0$. We consider the non-uniform internal heat generation/absorption in the flow to get the temperature and concentration differences between the surface and the ambient fluid. We assume that the velocity is proportional to its distance from the slit. Under the usual boundary layer approximation, the governing equations describing the momentum, energy and concentration in the presence of radiation, thermophoresis and other important parameters take the following form:
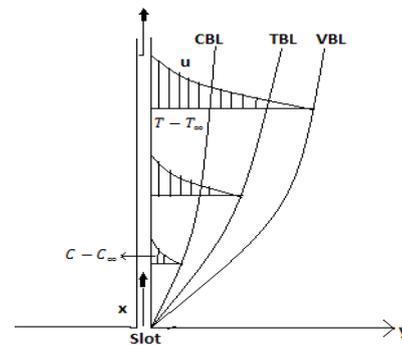
Fig. 1. Flow configuration and coordinate system.

$$\frac{\partial u}{\partial x} + \frac{\partial v}{\partial y} = 0 \tag{1}$$

$$\rho\left(\frac{\partial u}{\partial t} + u\frac{\partial u}{\partial x} + v\frac{\partial u}{\partial y}\right) = \mu\frac{\partial^2 u}{\partial y^2} - \frac{v}{k^1}u - \sigma B_0^2 u \tag{2}$$

$$\frac{\partial T}{\partial t} + u\frac{\partial T}{\partial x} + v\frac{\partial T}{\partial y} = \frac{\kappa}{\rho c_p}\frac{\partial^2 T}{\partial y^2} - \frac{1}{\rho c_p}\frac{\partial q_r}{\partial y}$$

$$+ \frac{1}{\rho c_p}(q''') + \frac{D_m k_T}{c_s c_p}\frac{\partial^2 C}{\partial y^2} \tag{3}$$

$$\frac{\partial C}{\partial t} + u\frac{\partial C}{\partial x} + v\frac{\partial C}{\partial y} = D_m\frac{\partial^2 C}{\partial y^2}$$

$$+\frac{D_m k_T}{T_m}\frac{\partial^2 T}{\partial y^2} - \frac{\partial}{\partial y}(V_T C) \qquad (4)$$

The associated boundary conditions are

$$u = U_w(x,t), \qquad v = V_w, \qquad T = T_w(x,t),$$
$$C = C_w(x,t),$$

at y = 0, $\qquad\qquad\qquad\qquad\qquad\qquad$ (5)

$$u \to 0, \ T \to T_\infty, \ C \to C_\infty, \quad as \ y \to \infty. \qquad (6)$$

where u and v are the components of velocity along x and y directions, respectively and t is the time. $U_w(x,t)$ is the stretching sheet velocity, $T_w(x,t)$ is the stretching surface temperature, $C_w(x,t)$ is the concentration of the stretching surface, T_∞ is the temperature far away from the stretching surface with $T_w > T_\infty$, C_∞ is the concentration far away from the stretching surface with $C_w > C_\infty$. The term $V_w = -\sqrt{\frac{vU_w}{2x}}f(0)$ represents the mass transfer at the surface with $V_w <$ 0 for suction and $V_w > 0$ for injection.

The non-uniform heat source/sink, q''', is defined as
$$q''' = \frac{\kappa U_w(x,t)}{xv}(A_1(T_w - T_\infty)f' + (T - T_\infty)B_1]$$

where A_1 and B_1 are the coefficients of space and temperature-dependent heat source/sink, respectively. The case $A_1 > 0$, $B_1 > 0$ corresponds to internal heat source and the case $A_1 < 0$, $B_1 < 0$ corresponds to internal heat sink.

Due to stretching of the sheet the flow is caused and it moves with the surface velocity, temperature and concentration of the form

$$U_w(x,t) = \frac{ax}{1 - ct}, \ T_w(x,t) = T_\infty + \frac{ax}{1 - ct},$$

$$C_w(x,t) = C_\infty + \frac{ax}{1-ct} \qquad (7)$$

where a (stretching rate) and c are positive constants with $ct < 1, c \geq 0$. It is noticed that the stretching rate $\frac{a}{1-ct}$ is increases with time t since $a > 0$.

The following similarity transformations (2009) are introduced to simplify the mathematical analysis of the problem

$$Ⴍ = \eta = \sqrt{\frac{a}{v(1-ct)}}\,y, u = \frac{ax}{1-ct}f'(\eta), v =$$

$$-\sqrt{\frac{va}{1-ct}}\,f(\eta) \qquad (8)$$

$$\theta(\eta) = \frac{T-T_\infty}{T_w-T_\infty}, \ \phi(\eta) = \frac{C-C_\infty}{C_w-C_\infty}. \qquad (9)$$

By using the Rosseland approximation for radiation, the radiative heat flux q_r is defined as

$$q_r = -\frac{4\sigma^*}{3K^*}\frac{\partial T^4}{\partial y}, \qquad (10)$$

where σ^* is the Stephan-Boltzman constant, K^* is the mean absorption coefficient. We assume that the temperature differences within the flow are such

that the term T^4 may be expressed as a linear function of temperature. This is accomplished by expanding T^4 in a Taylor series about a free stream temperature T_∞ as follows:

$$T^4 = T_\infty^{\ 4} + 4T_\infty^{\ 3}(T - T_\infty)$$

$$+6T_\infty^{\ 2}(T - T_\infty)^2 + \cdots \qquad (11)$$

Neglecting higher-order terms (9) in the above Eq. (11) beyond the first degree in $(T - T_\infty)$, we get

$$T^4 \cong 4T_\infty^{\ 3}T - 3T_\infty^{\ 4}. \qquad (12)$$

Thus substituting Eq. (12) in Eq.(10), we get

$$q_r = -\frac{16T_\infty^{\ 3}\sigma^*}{3K^*}\frac{\partial T}{\partial y}. \qquad (13)$$

The effect of thermophoresis is usually prescribed by means of an average velocity acquired by small particles to the gas velocity when exposed to a temperature gradient. In boundary layer flow, the temperature gradient in y-direction is very much larger than in the x-direction and therefore only the thermophoretic velocity in y-direction is considered. As a consequence, the thermophoretic velocity V_T, which appears in Eq. (5), is expressed as

$$V_T = -\frac{k_1 v}{T_r}\frac{\partial T}{\partial y} \qquad (14)$$

in which k_1 is the thermophoretic coefficient and T_r is the reference temperature. A thermophoretic parameter τ is given by the relation

$$\tau = -\frac{k_1(T_w - T_\infty)}{T_r} \qquad (15)$$

where the typical values of τ are 0.01, 0.1and 1.0 corresponding to approximate values of–$k_l(T_w$ - $T_\infty)$

equal to 3, 30, 300K for a reference temperature of T=298.15K.

Using Eqs. (8),(9),(13) and (15), the governing equations Eqs. (2) – (6) takes the form

$$f''' + ff'' - f'^2 - \alpha\left(f' + \frac{1}{2}\eta f''\right) - Mf' - kf' = 0 \qquad (16)$$

$$\left(1 + \frac{4}{3}An\right)\theta'' + Pr(f\theta' - f'\theta) - Pr\,\alpha\left(\theta + \frac{1}{2}\eta\theta'\right) + (A_1 f' + B_1\theta) + Du\,\phi'' = 0 \qquad (17)$$

$$\phi'' - Sc\,(2f'\phi - f\phi') - Sc\,\alpha\left(\phi + \frac{1}{2}\eta\phi'\right) + Sc\,Sr\,\theta'' - \tau(\theta'\phi' + \theta''\phi) = 0$$

$$\qquad (18)$$

The boundary conditions take the form

$$f = f_w, \ f' = 1, \ \theta = 1, \ \phi = 1 \ at\,\eta = 0,$$
$$\qquad (19)$$

$$f' = 0, \quad \theta = 0, \quad \phi = 0, \quad at\,\eta \to \infty \quad (20)$$

where Pr is the Prandtl number, An is the radiation parameter, α is the unsteadiness parameter, M is the magnetic field parameter, k is the permeability parameter, Sr is the Soret parameter, Du is the Dufour parameter, τ is the thermophoresis

parameter, Sc is the Schmidt number, $f(0) = f_w$ with $f_w > 0$ corresponds to suction and $f_w < 0$ represents injection.

Quantities of practical interest in this problem are the local skin friction coefficient C_f, the local Nusselt number Nu_x, and the local Sherwood number Sh_x, are defined as

$$C_f = \frac{\tau_w}{\rho U_w^2/2}, Nu_x = \frac{x\, q_w}{\kappa(T_w - T_\infty)}, \; Sh_x = \frac{x\, J_w}{D_m(C_w - C_\infty)}.$$

Here τ_w, q_w, and J_w are the wall shear stress, surface heat flux and the mass flux, respectively.

Using (8) and (9), we obtain the dimensionless versions of these key design quantities:

$$C_f = \frac{f''(0)}{Re_x^{\frac{1}{2}}}, \; Nu_x = -\theta'(0)Re_x^{\frac{1}{2}}, \; Sh_x = -\varphi'(0)Re_x^{\frac{1}{2}}.$$

Since the highly non-linear nature of ordinary differential Eqs. (16)–(18) together with boundary conditions (19)-(20), they cannot be solved analytically. So the variational finite-element method, Bhargava *et al.* (2009), Anwar Beg *et al.* (2008) and Rana. P *et al.* (2012) has been implemented.

3. NUMERICAL METHOD OF SOLUTION

3.1. The finite-element method

The finite element method (FEM) is such a powerful method for solving ordinary differential equations and partial differential equations. The basic idea of this method is dividing the whole domain into smaller elements of finite dimensions called finite elements. This method is such a good numerical method in modern engineering analysis, and it can be applied for solving integral equations including heat transfer, fluid mechanics, chemical processing, electrical systems, and many other fields. The steps involved in the finite-element are as follows.

(i) Finite-element discretization

The whole domain is divided into a finite number of subdomains, which is called the discretization of the domain. Each subdomain is called an element. The collection of elements is called the finite-element mesh.

(ii) Generation of the element equations

a. From the mesh, a typical element is isolated and the variational formulation of the given problem

over the typical element is constructed.

b. An approximate solution of the variational problem is assumed, and the element equations are

made by substituting this solution in the above system.

c. The element matrix, which is called stiffness matrix, is constructed by using the element

interpolation functions.

(iii) Assembly of element equations

The algebraic equations so obtained are assembled by imposing the interelement continuity conditions. This yields alarge number of algebraic equations known as the global finite-element model, which governs the whole domain.

(iv) Imposition of boundary conditions

The essential and natural boundary conditions are imposed on the assembled equations.

(v) Solution of assembled equations

The assembled equations so obtained can be solved by any of the numerical techniques, namely, the Gauss eliminationmethod, LU decomposition method, etc. An important consideration is that of the shape functions which are employed toapproximate actual functions.

For the solution of system non-linear ordinary differential Eqs. (16-18) together with boundary conditions (19-20), first we assume that

$$\frac{df}{d\eta} = h \tag{21}$$

The Eqs. (16) to (18) then reduces to

$$h'' + fh' - h^2 - \alpha\left(h + \frac{1}{2}\eta\, h'\right) - (M + K)h = 0 \tag{22}$$

$$\left(1 + \frac{4}{3}An\right)\theta'' + Pr(f\,\theta' - h\,\theta) - Pr\,\alpha\left(\theta + \frac{1}{2}\eta\,\theta'\right) + (A_1\,h + B_1\,\theta) + Du\,\phi'' = 0 \tag{23}$$

$$\phi'' - Sc\,(2\,h - f\,\phi') - Sc\,\alpha\left(\phi + \frac{1}{2}\eta\,\phi'\right) + Sc\,Sr\,\theta'' - \tau(\theta'\phi' + \theta''\phi) = 0 \tag{24}$$

The boundary conditions take the form

$$f = f_w, \quad h = 1, \quad \theta = 1, \quad \phi = 1 \quad at\, \eta = 0, \tag{25}$$
$$h = 0, \qquad \theta = 0, \qquad \phi = 0, \quad at\, \eta = \infty. \tag{26}$$

It has been observed that for large values of ($>$ 8), there is no remarkable change in the profiles, so, for computational purpose infinity has been taken as 8.

3.2. Variational Formulation

The variational form associated with Eqs. (21) to (24) over a typical linear element (η_e, η_{e+1}) is given by

$$\int_{\eta_e}^{\eta_{e+1}} w_1\left(\frac{df}{d\eta} - h\right)d\eta = 0 \tag{27}$$

$$\int_{\eta_e}^{\eta_{e+1}} w_2\left(h'' + fh' - h^2 - \alpha\left(h + \frac{1}{2}\eta\, h'\right) - (M + K)\,h\right)d\eta = 0 \tag{28}$$

$$\int_{\eta_e}^{\eta_{e+1}} w_3\left(\left(1 + \frac{4}{3}An\right)\theta'' + Pr(f\,\theta' - h\,\theta)\right.$$
$$- Pr\,\alpha\left(\theta + \frac{1}{2}\eta\,\theta'\right)$$
$$\left. + (A_1 h + B_1\theta) + Du\phi''\right)d\eta = 0 \tag{29}$$

$$\int_{\eta_e}^{\eta_{e+1}} w_4 \left(\phi'' - Sc\, (2\,h - f\, \phi') \right.$$

$$- Sc\ \alpha \left(\phi + \frac{1}{2} \eta\, \phi' \right)$$
$$+ Sc\, Sr\, \theta''$$
$$\left. - \tau \left(\theta' \phi' + \theta'' \phi \right) \right) d\eta = 0$$

$$(30)$$

where w_1, w_2, w_3 and w_4 are arbitrary test functions and may be viewed as the variations in *f*, *h*, *θ*, and *ϕ*, respectively.

3.3. Finite- Element Formulation

The finite-element model may be obtained from above equations by substituting finite-element approximations of the form

$$f = \sum_{j=1}^{3} f_j \psi_j\ ,\ h = \sum_{j=1}^{3} h_j \psi_j\ , \theta = \sum_{j=1}^{3} \theta_j \psi_j\ ,$$

$$\phi = \sum_{j=1}^{3} \phi_j \psi_j \qquad\qquad (31)$$

with $w_1 = w_2 = w_3 = w_4 = \psi_i, \qquad (i = 1,2,3).$

where ψ_i are the shape functions for a typical element (η_e, η_{e+1}) and are defined as

$$\psi_1^e = \frac{(\eta_{e+1}+\eta_e-2\,\eta)\,(\eta_{e+1}-\eta)}{(\eta_{e+1}-\eta)^2},$$

$$\psi_2^e = \frac{4(\eta-\eta_e)(\eta_{e+1}-\eta)}{(\eta_{e+1}-\eta)^2}\ , \qquad\qquad (32)$$

$$\psi_3^e = \frac{(\eta_{e+1}+\eta_e-2\,\eta)\,(\eta-\eta_e)}{(\eta_{e+1}-\eta)^2}, \eta_e \le \eta \le \eta_{e+1}.$$

The finite element model of the equations thus formed is given by

$$\begin{bmatrix} [K^{11}] & [K^{12}] & [K^{13}] & [K^{14}] \\ [K^{21}] & [K^{22}] & [K^{23}] & [K^{24}] \\ [K^{31}] & [K^{32}] & [K^{33}] & [K^{34}] \\ [K^{41}] & [K^{42}] & [K^{43}] & [K^{44}] \end{bmatrix} \begin{bmatrix} f \\ h \\ \theta \\ \phi \end{bmatrix} = \begin{bmatrix} \{r^1\} \\ \{r^2\} \\ \{r^3\} \\ \{r^4\} \end{bmatrix}$$

where $[K^{mn}]$ and $[r^m]$ (m, n = 1, 2, 3, 4) are defined as,

$$K_{ij}{}^{11} = \int_{\eta_e}^{\eta_{e+1}} \psi_i \frac{\partial \psi_j}{\partial \eta} d\eta, \qquad K_{ij}{}^{12} =$$

$$- \int_{\eta_e}^{\eta_{e+1}} \psi_i \psi_j\, d\eta, K_{ij}{}^{13} = K_{ij}{}^{14} = 0, \qquad K_{ij}{}^{21} =$$

$$\int_{\eta_e}^{\eta_{e+1}} \psi_i \bar{h} \psi_j\, d\eta,$$

$$K_{ij}{}^{22} = \int_{\eta_e}^{\eta_{e+1}} \left\{ -\frac{\partial \psi_i}{\partial \eta}\frac{\partial \psi_j}{\partial \eta} - \psi_i \bar{h}\psi_j - \alpha \left\{ \psi_i \psi_j + \right. \right.$$

$$\left. \left. \frac{1}{2}\eta\psi_i \bar{h}\psi_j \right\} \right\} d\eta - \int_{\eta_e}^{\eta_{e+1}} \psi_i (M + K)\psi_j d\eta\ ,$$

$$K_{ij}{}^{23} = 0\ , K_{ij}{}^{24} = 0\ ,$$

$$K_{ij}{}^{31} = Pr \int_{\eta_e}^{\eta_{e+1}} \psi_i \bar{\theta}\ \psi_j d\eta \qquad , \qquad K_{ij}{}^{32} =$$

$$- Pr \int_{\eta_e}^{\eta_{e+1}} \psi_i \psi_j d\eta + A_1 \int_{\eta_e}^{\eta_{e+1}} \psi_i \psi_j d\eta\ ,$$

$$K_{ij}{}^{33} = -\left(1 + \frac{4}{3}An \right) \int_{\eta_e}^{\eta_{e+1}} \frac{\partial \psi_i}{\partial \eta}\frac{\partial \psi_j}{\partial \eta}\ d\eta$$

$$+ Pr\, \alpha \int_{\eta_e}^{\eta_{e+1}} \psi_i (1 + \frac{1}{2}\eta\bar{\theta}$$

$$+ B_1)\psi_j\ d\eta$$

$$K_{ij}{}^{34} = Du \int_{\eta_e}^{\eta_{e+1}} \frac{\partial \psi_i}{\partial \eta}\frac{\partial \psi_j}{\partial \eta}\ d\eta.$$

$$K_{ij}{}^{41} = Sc \int_{\eta_e}^{\eta_{e+1}} \psi_i \bar{\phi}\, \psi_j\, d\eta, \qquad K_{ij}{}^{42} =$$

$$2\, Sc \int_{\eta_e}^{\eta_{e+1}} \psi_i \psi_j\, d\eta, \qquad K_{ij}{}^{43} =$$

$$Sc\, Sr \int_{\eta_e}^{\eta_{e+1}} \frac{\partial \psi_i}{\partial \eta}\frac{\partial \psi_j}{\partial \eta}\ d\eta + Sc\, \alpha \int_{\eta_e}^{\eta_{e+1}} \psi_i (1 +$$

$$\frac{1}{2}\eta\bar{\phi})\psi_j\ d\eta - \tau \int_{\eta_e}^{\eta_{e+1}} \psi_i \bar{\phi}\frac{\partial \psi_j}{\partial \eta}\ d\eta -$$

$$\tau \int_{\eta_e}^{\eta_{e+1}} \frac{\partial \psi_i}{\partial \eta}\frac{\partial \psi_j}{\partial \eta}\ d\eta, \qquad K_{ij}{}^{44} = \int_{\eta_e}^{\eta_{e+1}} \frac{\partial \psi_i}{\partial \eta}\frac{\partial \psi_j}{\partial \eta}\ d\eta.$$

$$r_i^2 = 0\ , r_i^2 = -\left(\psi_i \frac{d\psi_i}{d\eta} \right)_{\eta_e}^{\eta_{e+1}},\ r_i^3 = -\left(\psi_i \frac{d\psi_i}{d\eta} \right)_{\eta_e}^{\eta_{e+1}}$$

$$, r_i^4 = -\left(\psi_i \frac{d\psi_i}{d\eta} \right)_{\eta_e}^{\eta_{e+1}}$$

where

$$\bar{f} = \sum_{j=1}^{3} f_i \frac{\partial \psi_i}{\partial \eta}\, \bar{h} = \sum_{j=1}^{3} h_i \frac{\partial \psi_i}{\partial \eta}\ ,$$

$$\bar{\theta} = \sum_{j=1}^{3} \theta_i \frac{\partial \psi_i}{\partial \eta},\qquad \bar{\phi} = \sum_{j=1}^{3} \phi_i \frac{\partial \psi_i}{\partial \eta}.$$

After assembly of the element equations, we get the system of strongly non-linear equations and are solved using a robust iterative scheme. The system is linearized by incorporating the functions $\bar{f}, \bar{h}, \bar{\theta}$ and $\bar{\phi}$, which are assumed to be known. After imposing the boundary conditions, we get the less number of non-linear equations and are solved using Gauss elimination method by maintaining an accuracy of 0.00001. The computer program of the algorithm was executed in Mathematica 10.0 software.

4. RESULTS AND DISCUSSION

Comprehensive numerical computations are conducted for different values of the parameters that describe the flow characteristics, and the results are illustrated graphically and in tabular form. Selected graphical profiles are presented in Figs. 2-19. The Comparison of the skin friction coefficient $f''(0)$ for various values of αwith Dulal Pal (2011) is made and the results are shown in Table 1in the absence of the other parameters. The Nusselt number Nu_xvalues for various values of *Pr* and α are also compared with those of Ishak. A *et al*. [2009], Dulal Pal (2011) and Eshetu Haile *et al*. (2014)in the absence of *k, M, Sr, Du, A_1, B_1,Sc,f_w,τ*and are presented in Table 2. Thus, it is seen from Tables 1 and 2 that the numerical results are in close agreement with those published previously.

Table 1 Comparison of $f''(0)$ with previously published data for $k=0$, $M=0$, $Sr=0$, $Du=0$, $Sc=0$, $A_1=0$, $B_1=0$, $f_w=0$ and $\tau=0$

	$f''(0)$	
α	Dulal pal(2011)	Present Study
0.8	-1.261043	-1.261036
1.2	-1.377724	-1.377658
2.0	-1.587366	-1.587301

Table 2 Comparison of $-\theta'(0)$ with previously published data for $k=0$, $M=0$, $Sr=0$, $Du=0$, $Sc=0$, $A_1=0$, $B_1=0$, and $\tau=0$

			Nu_x			
α	f_w	Pr	Ishak.A.*et al.* (2009)	Dulal Pal (2011)	Haile.E.*et al.* (2014)	Present Study
0.0	0.0	1.0	1.0000	1.0000	1.0004	1.0002
0.0	0.0	3.0	1.9237	1.9236	1.9234	1.9235
0.0	0.0	10.0	3.7207	3.7207	3.7205	3.7205
0.0	0.0	100.0	12.2941	12.2940	12.2962	12.2948
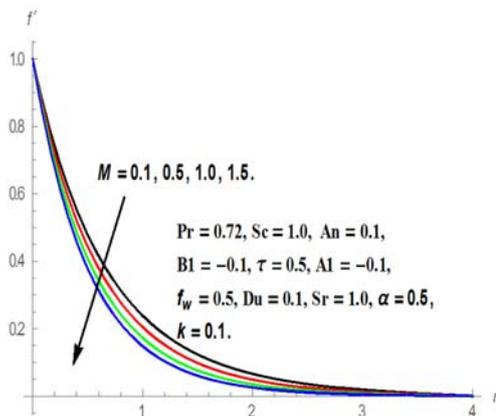
Fig. 2. Effect of M on Velocity profile.

This is because of the fact that, the presence of magnetic field in an electrically-conducting fluid produces a force called the Lorentz force which acts against the flow direction causing the depreciation Inthe velocity profiles (Fig. 2). We noticed from Figs. 3 and 4 that the temperature and concentration profiles are enhanced with increasing values of M. This is from the reality that, to overcome the drag force imposed by the Lorentz retardation, the fluid has to perform extra work and this supplementary work can be converted into thermal energy which increases the temperature and concentration of the fluid.

Figures 5 - 7 depict the velocity (f'), temperature (θ) and concentration (φ) distributions for different values of the suction parameter (f_w).It can be seen that as the values of suction parameter (f_w) increase the fluid velocity profiles decelerates in the boundary layer regime. This is due to the fact that suction takes away the warm fluid from

Fig. 3. Effect of M on temperature profile.

The influence of magnetic field parameter (M) on the velocity, temperature and concentration profiles in the boundary layer is depicted in Figs.2 to 4. It is noticed that the momentum boundary layer thickness decreases with increasing values of M.
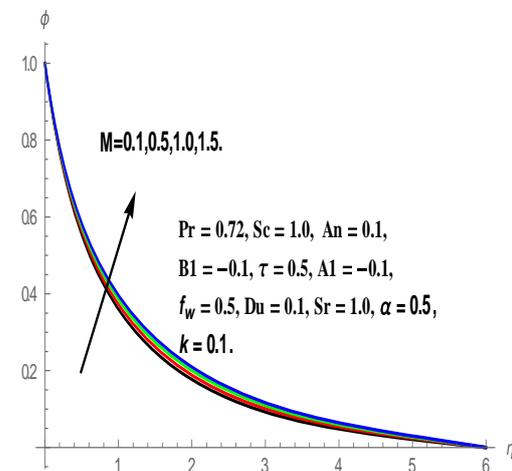
Fig. 4. Effect of M on Concentration profile.

the surface of the sheet and thereby decreases the thickness of hydrodynamic boundary layer (Fig.5). It is observed that an increase in (f_w) decreases the temperature profiles in the flow region. This is because of the fact that as the suction is increased, more warm fluid is taken away from the fluid region causing depreciation in the thermal boundary layer thickness (Fig.6). We notice from Fig. 7 that the concentration profiles decelerate with an increase in the suction parameter. This is because suction stabilizes the growth of the solutal boundary layer thickness.

The concentration profiles also decreases in the flow region as shown in Fig. 9. It is also observed that the temperature profiles decrease smoothly in the absence of the unsteadiness parameter ($\alpha=0$) whereas the temperature profiles continuously depreciates with the increasing values of unsteadiness parameter. This shows that the rate of cooling is much faster for higher values of the unsteadiness parameter and it takes longer time for cooling for steady flows.

Fig. 5. Effect of f_w on Velocity profile.
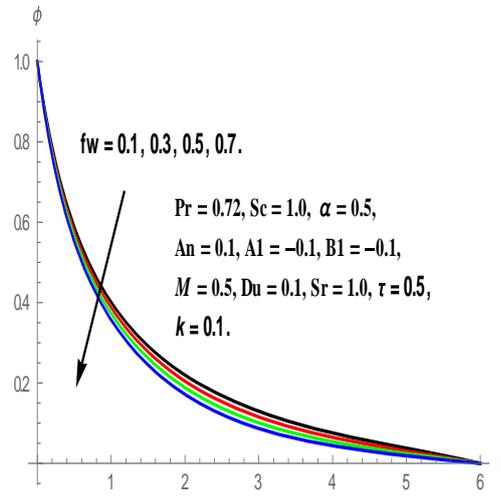
Fig. 7. Effect of f_w on Concentration profile.

Fig. 6. Effect of f_w on Temperature profile.

Fig. 8. Effect of α on Temperature profile.

The influence of unsteadiness parameter (α) on the temperature and the concentration profiles is depicted in Figs. 8-9. It can be seen that the temperature profiles decelerate with an increase in the values of the unsteadiness parameter α. This is because of the usual fact that, motion is generated by the stretching of the sheet and the stretching sheet velocity and temperature are greater than the free stream velocity and temperature. As a result, the thermal boundary layer thickness decreases with the increase in the value of α as shown in Fig. 8.

Fig. 9. Effect of α on Concentration profile.

Fig. 10. Effect of τ on Temperature profile.

The effects of the thermophoretic parameter τ on the temperature and the concentration profiles are plotted in Figs. 10 and 11. It is seen from Fig.10 that an increase in the value of τ there exist a slight enhancement in the temperature profiles throughout the fluid regime. This is because of the fact that the particles near the hot surface create a thermophoretic force. Fig.11 exhibits the impact of τ on the concentration profiles. It is noticed that the concentration profiles decrease with an increase in the thermophoretic parameter τ. This is because the fluid moves from the hot surface to the cold surface and that the values of the thermophoretic parameter have been taken positive. From these two figures, we conclude that the imposition of thermophoretic particle deposition into the flow increases the thickness of thermal boundary layer and decreases the solutal boundary layer thickness.
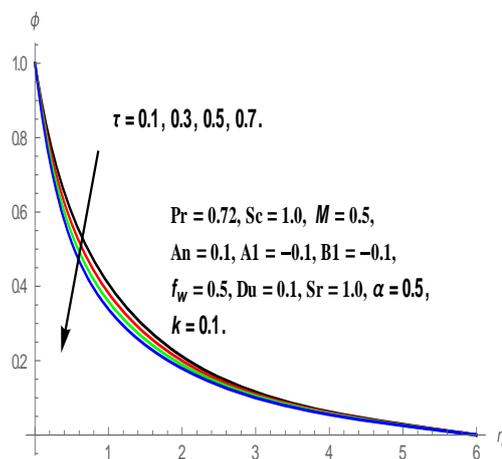
Fig. 11. Effect of τ on concentration profile.

The temperature and concentration profiles for different values of the space-dependent and temperature-dependent coefficients A1 and B1 for the heat source/sink are depicted in Figs.12 to15.It is observed that the temperature in the thermal boundary layer increases with the increase in A1and B1 (positive values), whereas the thermal boundary layer thickness decelerates with the decrease in the

heat absorption parameters A1 and B1 (negative values). This is due to the fact that with increases in A1>0, B1>0(heat source), the boundary layer creates energy which causes a rise in the temperature profile, whereas, with decreases in A1< 0, B1< 0(heat absorption), the boundary layer absorbs the energy so that the thermal boundary layer thickness decreases in the fluid regime as shown in Figs.12 and 14.The exact reverse trend is noticed on the concentration profiles with the space-dependent and temperature-dependent coefficients A_1 and B_1 for both heat generation and heat absorption cases and this behavior is presented in Figs. 13 and 15.
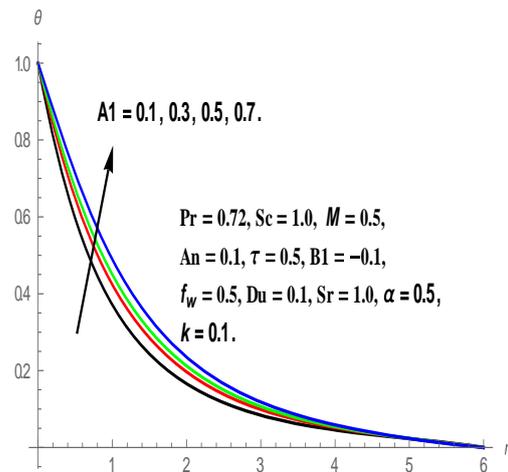
Fig. 12. Effect of A1 on Temperature profile.
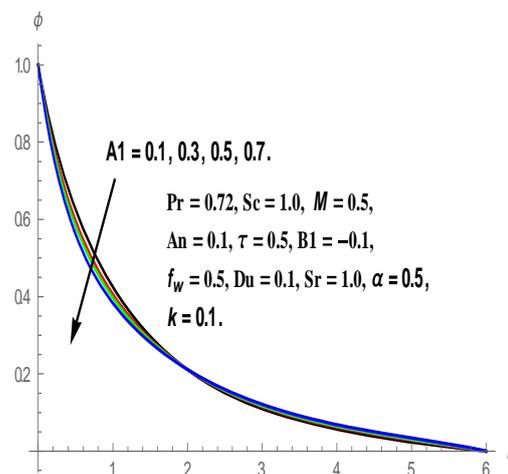
Fig. 13. Effect of A1 on Concentration profile.

The combined influence of thermo-diffusion (Soret) and the diffusion-thermo (Dufour) effects on the temperature and the concentration profiles are plotted in Figs.16 and 17, respectively. The values of Sr and Du have been taken as Sr = 1.0, 0.7,0.4,0.1 and Du = 0.1, 0.3, 0.5,0.7, i.e. the Soret parameter values decrease and the Dufour parameter values increase. It is seen from these figures that the temperature profiles increase, whereas the concentration profiles decelerate with the rise in Du and the fall in Sr. From the

definition, the Soret number can be defined as the effect of the temperature on the concentration and the Dufour number can be defined as the effect of the concentration on the temperature. This shows that diffusive species with lower Soret values decelerate the concentration profiles whereas the thermal species with higher Dufour values have the tendency of increasing the temperature profiles. It is worth noticing that both the heat and mass transfer are highly influenced by the changes in Sr and Du.
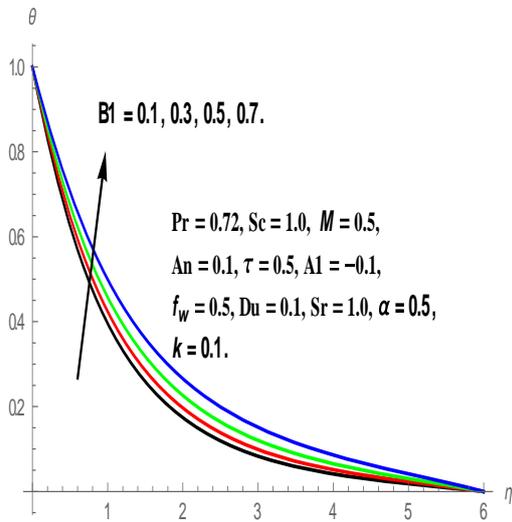
Fig. 14. Effect of *B*1 on Temperature profile.
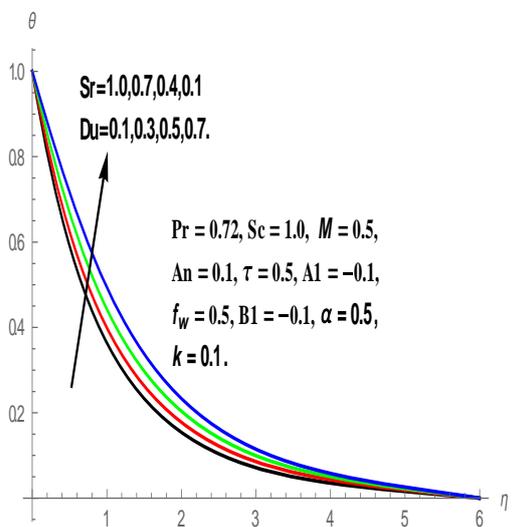
Fig. 16. Effect of *Sr* and *Du* on Temperature profile.

Figures. 18 and 19 present the effects of the thermal radiation parameter An on the temperature and the concentration distributions. It is observed form Fig. 18 that as the values of An increase, the thickness of the thermal boundary layer also increases. This is due to the fact that imposition of An in the fluid flow implies increasing of the thermal radiation in the thermal boundary layer which results in an

increase in the value of the temperature profile in the fluid regime. However, reverse trend is observed in the solutal boundary layer thickness with increasing values of An in the flow region and this is shown in Fig. 19.
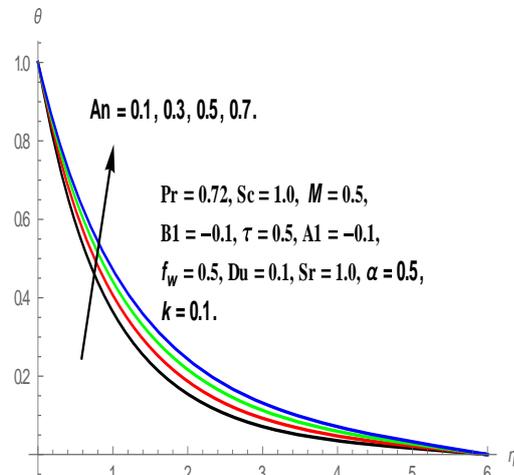
Fig. 18. Effect of *An* on Temperature profile.
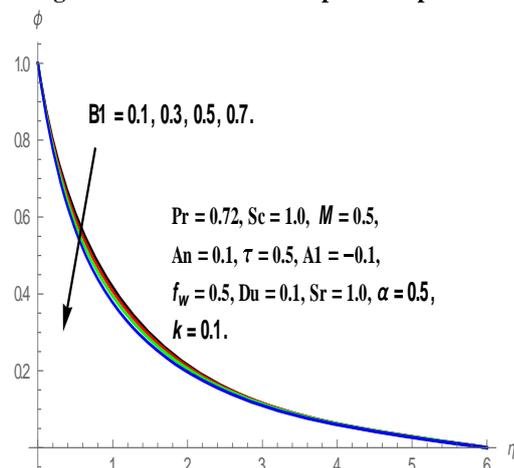
Fig. 15. Effect of B1 on Concentration profile.
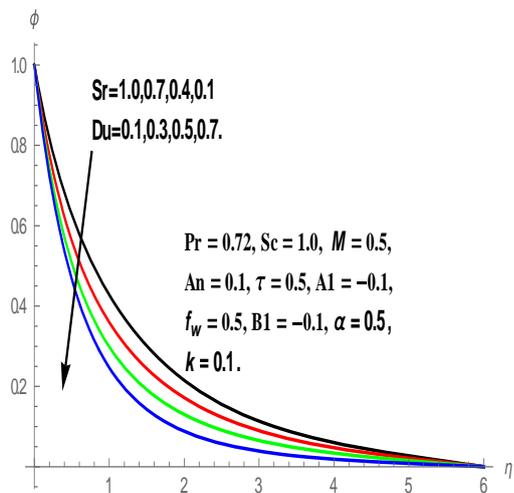
Fig. 17. Effect of *Sr* and *Du* on Concentration profile.

2452

Table 3 The local Skin-friction, Nusselt number and Sherwood number for different values of the important parameters

M	f_w	A1	B1	Sr	Du	τ	An	$f''(0)$	$-\theta'(0)$	$-\phi'(0)$
0.1	0.5	-0.1	-0.1	1.0	0.1	0.5	0.1	−1.5158744	1.0954583	1.4353078
0.5	0.5	-0.1	-0.1	1.0	0.1	0.5	0.1	−1.6666449	1.0769383	1.4044462
1.0	0.5	-0.1	-0.1	1.0	0.1	0.5	0.1	−1.8346139	1.0581713	1.3724033
1.5	0.5	-0.1	-0.1	1.0	0.1	0.5	0.1	−1.9860796	1.0427808	1.3455601
0.5	0.1	-0.1	-0.1	1.0	0.1	0.5	0.1	−1.4519989	0.9558400	1.2787791
0.5	0.3	-0.1	-0.1	1.0	0.1	0.5	0.1	−1.5557482	1.0142059	1.3398008
0.5	0.5	-0.1	-0.1	1.0	0.1	0.5	0.1	−1.6666449	1.0769383	1.4044462
0.5	0.7	-0.5	-0.1	1.0	0.1	0.5	0.1	−1.7845786	1.1440810	1.4731732
0.5	0.5	-0.1	-0.1	1.0	0.1	0.5	0.1	−1.3363316	1.0638213	1.0989064
0.5	0.5	0.1	-0.1	1.0	0.1	0.5	0.1	−1.3257839	0.8488358	1.2599294
0.5	0.5	0.5	-0.1	1.0	0.1	0.5	0.1	−1.3704027	0.7413729	1.3403629
0.5	0.5	-0.1	-0.1	1.0	0.1	0.5	0.1	−1.4023647	0.5802159	1.4609154
0.5	0.5	-0.1	-0.3	1.0	0.1	0.5	0.1	−1.1278748	0.9273635	1.2046987
0.5	0.5	-0.1	-0.1	1.0	0.1	0.5	0.1	−1.2578397	0.8488358	1.2599294
0.5	0.5	-0.1	0.1	1.0	0.1	0.5	0.1	−1.6594641	0.7619111	1.3199523
0.5	0.5	-0.1	0.2	1.0	0.1	0.5	0.1	−1.7868723	0.6631123	1.3865907
0.5	0.5	-0.1	-0.1	1.0	0.1	0.5	0.1	−1.2867381	1.0967356	1.0738634
0.5	0.5	-0.1	-0.1	0.7	0.3	0.5	0.1	−1.3188963	0.9541261	1.3445090
0.5	0.5	-0.1	-0.1	0.4	0.5	0.5	0.1	−1.3748052	0.7670185	1.5553249
0.5	0.5	-0.1	-0.1	0.1	0.7	0.5	0.1	−1.3549166	0.5721138	1.6720642
0.5	0.5	-0.1	-0.1	1.0	0.1	0.1	0.1	−1.3257839	0.8488358	1.2599294
0.5	0.5	-0.1	-0.1	1.0	0.1	0.3	0.1	−1.3203397	0.8052550	1.4059782
0.5	0.5	-0.1	-0.1	1.0	0.1	0.5	0.1	−1.2341730	0.7661899	1.5370934
0.5	0.5	-0.1	-0.1	1.0	0.1	0.7	0.1	−1.2120002	0.7309419	1.6555676
0.5	0.5	-0.1	-0.1	1.0	0.1	0.5	0.1	−1.2867381	1.0967356	1.0738634
0.5	0.5	-0.1	-0.1	1.0	0.1	0.5	0.3	−1.2693179	0.9772594	1.1582161
0.5	0.5	-0.1	-0.1	1.0	0.1	0.5	0.5	−1.245810	0.8866948	1.2208495
0.5	0.5	-0.1	-0.1	1.0	0.1	0.5	0.7	−1.2267640	0.8153569	1.2693241
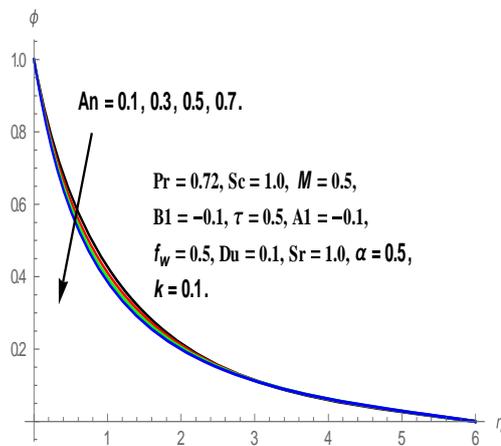
Fig. 19. Effect of *An* on Concentration profile.

An = 0.1, 0.3, 0.5, 0.7.

Pr = 0.72, Sc = 1.0, *M* = 0.5,
B1 = −0.1, τ = 0.5, A1 = −0.1,
f_w = 0.5, Du = 0.1, Sr = 1.0, *α* = 0.5,
k = 0.1.

The variation of the local skin-friction coefficient $f''(0)$, local Nusselt number $-\theta'(0)$, and the local Sherwood number $-\phi'(0)$ for different values of the important parameters are presented in Table 3. It is evident that all these non-dimensional rate coefficients decelerate with increasing values of the magnetic parameter M. Further, it is noted that the rates of the velocity depreciates, whereas the rates of the dimensionless heat transfer and rates of the dimensionless mass transfer enhance with increasing values of the suction ($f_w > 0$) parameter. It is observed from this table that the effects of the space dependent (A1) and the temperature-dependent (B1) parameters are similar on these non-dimensional rate coefficients. Moreover, the rates of non-dimensional velocity and heat transfer decrease whereas the rates of the non-dimensional mass transfer enhances for the values of both A1 and B1. The effect of the Soret parameter Sr together with the Dufour parameter Du on these non-dimensional rate coefficients is also shown in the table and it is observed that $f''(0)$ and $-\theta'(0)$ decelerate, whereas $-\phi'(0)$ enhances in the flow region. The influence of thermophoretic parameter τ and thermal radiation parameter *An* is similar on these non-dimensional rate coefficients. It can be noted that the local skin-friction coefficient and the local Sherwood number increase whereas the Nusselt number decreases with increasing values of τ and An.

5. CONCLUSION

In this paper, the problem of unsteady boundary layer, heat and mass transfer flow of a viscous incompressible electrically-conducting fluid through porous medium over a stretching sheet subject to thermal radiation, magnetic field, heat source/sink, Soret effect, Dufour effect and thermophoresis effect has been analyzed. The governing highly non-linear partial differential equations together with the boundary conditions are transformed into non-linear ordinary differential equations using the similarity variables and these are solved with the help of the variational finite-element method. The numerical results show that

the present values of the local skin-friction coefficient and the Nusselt number are in good agreement with previously published work. In the present analysis, the following conclusions have attained.

(i) The velocity, temperature and the concentration profiles decrease with increases in the suction parameter, satisfying the fact that suction decelerates the momentum, thermal and solutal boundary layer thickness.

(ii) Increasing the Lorentz force decreases the velocity of the fluid.

(iii) The momentum, thermal and the concentration profiles decrease with increases in the unsteadiness parameter.

(iv) The effect of the Soret number enhances the rate of heat transfer, whereas it decelerates the rate of mass transfer.

(v) The Nusselt number decreases whereas the Sherwood number increases with increases in the values of the thermal radiation parameter.

(vi) The effect of space-dependent and temperature-dependent heat source/sink is same on both the Nusselt number and the Sherwood number.

ACKNOWLEDGMENTS

REFERENCES

Abo-Eldahab, E. M. and M. S. El-Gendy (2004). Heat current and Ohmic heating effect on mixed convection boundary layer flow of a micropolar fluid from a rotating cone with power-law variation in surface temperature.*Int. Commun. Heat Mass Transfer31, 751–762.*

Ali, M. E (1994). Heat transfer characteristics of a continuous stretching surface. *Heat Mass Transfer 29, 227–234.*

Anwar Bég, O., H. S.Takhar, R. Bhargava, S. Rawat and V. R. Prasad (2008). Numerical study of heat transfer of a third grade viscoelastic fluid in non-Darcian porous media with thermo physical effects. *Phys. Scr 77, 1–11.*

Bhargava, R, R. Sharma and O. A. Bég (2009). Oscillatory chemically-reacting MHD free convection heat and mass transfer in a porous medium with Soret and Dufour effects, finite element modeling. *Int. J. Appl. Math. Mech 5(6),15–37.*

Chamkha, A. J. and A. M. Rashad (2014). Unsteady heat and mass transfer by MHD mixed convection flow from a rotating verticalcone with chemical reaction and Soret and Dufour effects. *The Canadian Journal of Chemical Engineering.*

Chamkha, A. J. and A. M. Aly (2011a). MHD Free Convection Flow of a Nanofluid past a Vertical Plate in the Presence of Heat Generation or Absorption Effects. *Chemical Engineering Communications 198, 425-441.*

Chamkha, A. J. and S. E. Ahmed (2011b). Similarity Solution for Unsteady MHD Flow Near a Stagnation Point of a Three-Dimensional Porous Body with Heat and Mass Transfer, Heat Generation/Absorption and Chemical Reaction. *Journal of Applied Fluid Mechanics 4(2), 87-94.*

Chamkha, A. J., A. M. Aly and M. A. Mansour (2010). Similarity Solution for Unsteady Heat and Mass Transfer from a Stretching Surface Embedded in a Porous Medium with Suction/Injection and Chemical Reaction Effects. *Chemical Engineering Communications 197, 846-858.*

Chamkha, A. J., H. S. Takhar and V. M. Soundalgekar (2001). Radiation Effects on Free Convection Flow Past a Semi-Infinite Vertical Plate with Mass Transfer. *Chemical Engineering Journal 84, 335-342.*

Crane, L.J. (1970). Flow past a stretching plate. Z. Angew. *Math. Phys 21,645–647.*

Damseh, R. A., M. S. Tahat and A. C. Benim (2009). Non-similar solutions of magnetohydrodynamic and thermophoresis particle deposition on mixed convection problem in porous media along a vertical surface with variable wall temperature. *Progress in Computational Fluid Dynamics 9(1), 58-65.*

Dinesh, K. K. and S. Jayaraj (2009). Augmentation of thermophoretic deposition in natural convection flow through a parallel plate channel with heat sources. *Int. Communications Heat and Mass Transfer 36, 931–935.*

Dulal, P. (2011). Combined effects of non-uniform heat source/sink and thermal radiation on heat transfer over an unsteady stretching permeable surface. *Commun Nonlinear Sci Numer Simulat 16, 1890–1904.*

Dulal, P. and H. Mondal (2014). Soret-Dufour Effects on Hydromagnetic Non-Darcy Convective-Radiative Heat and Mass Transfer over a Stretching Sheet in Porous Medium with Viscous Dissipation and Ohmic Heating. *Journal of Applied Fluid Mechanics 7(3), 513-523.*

Duwairi, H. M. and R. A. Damseh (2008). Effect of thermophoresis particle deposition on mixed convection from vertical surfaces embedded in saturated porous medium. *Int. J. Numerical Methods Heat Fluid Flow18 (2), 202-216.*

Elbashbeshy, E. M. A. and M. A. A.Bazid (2004). Heat transfer over an unsteady stretching surface. *Heat Mass Transfer 41,1–4.*

Eshetu, H. and B. Shankar (2014).Heat and Mass Transfer in the Boundary Layer of Unsteady Viscous Nano fluid along a Vertical Stretching Sheet.*Journal of Computational Engineering.*

Grosan, T., R. Pop and I. Pop (2009). Thermophoretic deposition of particles in fully developed mixed convection flow in a parallel plate vertical channel. *Heat Mass Transfer 45, 503–509.*

Grubka, L. G. and K. M. Bobba (1985). Heat transfer characteristics of a continuous stretching surface with variable temperature. *J. Heat Transfer — Trans. ASME 107, 248–250.*

Gupta, P. S. and A. S. Gupta (1977). Heat and mass transfer on a stretching sheet with suction or blowing. *Can. J. Chem. Eng 55, 744–746.*

Ishak, A. (2010). Unsteady MHD flow and heat transfer over a stretching plate. *J. Applied Sci 10(18), 2127-2131.*

Ishak, A., R. Nazar and I. Pop (2009). Heat transfer over an unsteady stretching permeable surface with prescribed wall temperature. *Nonlinear Anal: Real World Appl 10, 2909–13.*

Ishak, A., R. Nazar and I. Pop (2009). Boundary layer flow and heat transfer over an unsteady stretching vertical surface. *Meccanica 44, 369–375.*

Liu, Z., Z. Chen and M. Shi (2009). Thermophoresis of particles in aqueous solution in micro-channel. *Applied Thermal Engineering 29(5-6), 1020–1025.*

Mahdy, A. and F. M. Hady (2009). Effect of thermophoretic particle deposition in non-Newtonian free convection flow over a vertical plate with magnetic field effect. *Journal of Non-Newtonian Fluid Mechanics 161(1-3), 37-41.*

Makinde. O. D. (2011). On MHD Mixed Convection with Soret and Dufour Effects Past a Vertical Plate Embedded in a Porous Medium. *Latin American Applied Research 41, 63-68.*

Mansour, M. A. and N. A. El-Shaer (2001). Radiative effects on magnetohydrodynamic natural convection flows saturated in porous media. *J. Magn. Magn. Mater 237, 327–341.*

Molla, M. M., S. C. Saha and M. A. Hossain (2011). Radiation effect on free convection laminar flow along a vertical flat plate with stream wise sinusoidal surface temperature. *Math. Comput. Modeling 53,1310–1319.*

Pal, D. (2005). Heat and mass transfer in stagnation-point flow towards a stretching surface in the presence of buoyancy force and thermal radiation. *Meccanica 44,145–158.*

Pal, D. and H. Mandal (2010). The influence of thermal radiation on hydromagnetic Darcy–Forchheimer mixed convection flow past a stretching sheet embedded in a porous medium. *Meccanica.*

Plumb, O. A., J. S. Huenfeld and E. J. Eschbach (1981). The effect of cross flow and radiation on natural convection from vertical heated surfaces in saturated porous media. *AIAA 16th Thermophysics Conference, June 23–25, Palo Alto, California, USA.*

Postelnicu, A. (2007). Effects of thermophoresis particle deposition in free convection boundary layer from a horizontal flat plate embedded in a porous medium. *Int. J. Heat Mass Transfer 50(15-16), 2981–2985.*

Rana, P. and R. Bhargava (2012). Flow and heat transfer of a Nano fluid over a nonlinearly stretching sheet: a numerical study. *Comm. Nonlinear Sci. Numer. Simulat 17, 212–226.*

Reddy, P. S. and V. P. Rao (2012). Thermo-Diffusion and Diffusion –Thermo Effects on Convective Heat and Mass Transfer through a Porous Medium in a Circular Cylindrical Annulus with Quadratic Density Temperature Variation–Finite Element Study.*Journal of Applied Fluid Mechanics 5(4), 139-144.*

Sakiadis, B. C. (1961). Boundary layer behavior on continuous solid surfaces. AIChE J.7, 26–28.

Talbot, L., R. K. Cheng and R. W. Schefer and *et al.* (1980). Thermophoresis of particles in a heated boundary layer. *J. Fluid Mech 101(4), 737–758.*

Tsai, R. and J. S. Huang (2010). Combined effects of thermophoresis and electrophoresis on particle deposition onto a vertical flat plate from mixed convection flow through a porous medium. *Chemical Eng. J. 157, 52–59.*

Tsai, R., K. H. Huang and J. S. Huang (2008). Flow and heat transfer over an unsteady stretching surface with non-uniform heat source.Int. Commun. *Heat Mass Transfer 35, 1340-1343.*

Tsou, F. K., E. M. Sparrow and R. J. Goldstein (1967). Flow and heat transfer in the boundary layer on a continuous moving surface. *Int. J. Heat Mass Transfer 10, 219–235.*

Vajravelu, K. (1994). Flow and heat transfer in a saturated porous medium over a stretching surface. Z. Angew. Math. *Mech 74,605–614.*

Vajravelu, K. and D. Rollins (1992). Heat transfer in electrically conducting fluid over a stretching surface. *Internat. J. Non-Linear Mech 27(2), 265–277.*

Wang, C. Y. (1990). Liquid film on an unsteady stretching surface. *Q Appl Math 48,601–10.*